Control of Crystallization and Melting Behavior in Sequence Specific Polypeptoids

Adrianne M. Rosales,[†] **Hannah K. Murnen,**[†] **Ronald N. Zuckermann,**[‡] **and Rachel A. Segalman**[*,†,§]

[†]*Department of Chemical Engineering,* [‡]*Molecular Foundry, Materials Science Division, Lawrence Berkeley National Laboratories, and* [§]*Materials Science Division, Lawrence Berkeley National Laboratories, University of California Berkeley, Berkeley, California 94720*

Received February 2, 2010; Revised Manuscript Received May 24, 2010

ABSTRACT: The sequence specificity of a class of biologically inspired polymers based on N-substituted glycines (polypeptoids) allows for a degree of tunability in the crystallization and thermal behavior not available in classical polymer systems. It is demonstrated that a series of peptoid homopolymers are stable up to temperatures of 250−300 °C and are crystalline with reversible melting transitions ranging from 150 to 225 °C. Defects inserted at precise locations along the polymer backbone (as monomer substitutions) enable control of the melting temperature. Melting points decrease with increased defect content, and X-ray diffraction (XRD) indicates defect inclusion in the crystal lattice. In addition, it is demonstrated that the distribution of the defects for a given content level affects the thermal properties of the peptoid chain.

Introduction

The ability to control the thermal processability and physical properties of polymers depends to a large extent on controlling their crystallization. While many processing variables can affect the rate of crystallization or percent crystallinity of a given polymer, inherent properties such as the melting temperature depend on the chemical nature of the polymer. One of the easiest routes to altering these properties is through copolymerization, with either a chemically dissimilar monomer or a structural isomer. The chemical or steric interaction of the specific monomer substitution or comonomer with the main chain can strongly influence the crystallinity and melting behavior.[1] A large and fascinating body of work with copolymers, polyethylenes in particular, has provided much insight into how the type, content, and distribution of the co-unit affect melting.[2−7] Although there is much theoretical interest in the effects of sequence distribution on copolymer melting,[8,9] experimental control of such systems has been difficult synthetically. Experimentally, the concept of introducing defects at precise locations in a polymer sequence and the subsequent effect on crystallinity is relatively unexplored.

In general, the introduction of a comonomer into a crystalline homopolymer chain presents two possible cases: the co-unit either enters the crystal lattice of the polymer chain or it is excluded from it. Flory developed the equilibrium theory of crystallization for the case in which the comonomer is excluded from the crystalline phase and essentially acts as a defect in the polymer chain, thereby depressing the melting point.[10,11] For this case, the melting temperature T_m of the copolymer can be given by

$$\frac{1}{T_m} = \frac{1}{T_m^0} - \frac{R \ln p}{\Delta H} \qquad (1)$$

where T_m^0 is the melting temperature of the pure homopolymer, ΔH is the enthalpy of fusion per monomer unit, and p is the probability that a crystallizable monomer is followed by another

such unit. The most well-studied case is that of purely random copolymers, in which p is equal to the mole fraction of crystallizable units (X). In agreement with the behavior predicted by Flory, several empirical studies have found a correlation between increasing comonomer content (decreasing X) and decreasing levels of crystallinity.[12−16] Much interest has also been focused on the role that the heterogeneity of the comonomer content distribution plays in the thermal properties of a copolymer.[3,17−19] Various stepwise DSC methods have been used to separate sequences of different comonomer content levels. Such DSC methods generally involve multiple annealing stages at decreasing temperature intervals to selectively crystallize copolymers of various compositions, which can then be detected upon the next heating run.[20] Despite the progress in narrowing comonomer distributions, there is still a lack of control in which these sequences can be specified in an exact, monodisperse fashion.

Recently, a level of sequence control has been achieved in which comonomer units are placed on every nth carbon along a polyethylene chain using acyclic diene metathesis (ADMET) polymerization.[21] These precision copolymers have provided insight into how the distribution of short alkyl branches along the chain affects melting behavior; namely, it was found that systems with precise comonomer placement tolerate a higher amount of defects compared to random systems before crystallinity is disrupted.[22,23] Bockstaller et al. performed similar experiments with halogenated comonomers and found that while both random and regularly placed comonomers depress the melting temperature, the resulting crystalline lamellae are different in morphology.[7,24] While these precision copolymers are a significant effort in understanding the interplay between polymer sequence and physical properties, greater control over defect placement and defect chemistry is clearly needed to gain further insight and to finely tune polymer properties.

In contrast to the systems studied above, biologically derived and biologically inspired polymers can be sequence-specific. Polypeptides of defined sequence can be synthesized by solid-phase synthesis methods and hold the potential to create systems
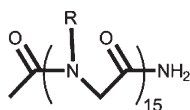
*To whom correspondence should be addressed.

Figure 1. Model acetylated peptoid 15-mer. R denotes side chain.

Table 1. N-Substituted Glycine Side Chains

Side Chain (R=)	Designator
	Nbu = N-(butyl)glycine
	Nhx = N-(hexyl)glycine
	Noc = N-(octyl)glycine
	Nia = N-(isoamyl)glycine
	Npe = N-(1-phenylethyl)glycine
	Nme = N-(2-methoxyethyl)glycine
	Npp = N-(3-phenyl-1-propyl)glycine

in which polymer primary structure can be manipulated to control polymer thermal properties. However, polypeptide thermal processability is poor due to the dominant effect of intra- and intermolecular hydrogen bonding on melting behavior. Alternatively, a variety of peptidomimetic oligomer systems allow access to a wide range of sequence-specific materials.[25] Of these, polypeptoids offer an ideal platform to explore thermal behavior due to their ease of synthesis and unique structure. Polypeptoids are based on an N-substituted glycine backbone (as shown in Figure 1)[26] and have simplified intermolecular interactions as compared to polypeptides and other peptidomimetic oligomers. Whereas peptide chains are dominated by hydrogen-bonding interactions, the N-substitution in peptoid polymers precludes the presence of hydrogen bond donors along the backbone. While most sequence-specific polymers require complex and low yielding synthetic routes, peptoids utilize a rapid, solid-phase submonomer synthetic method[26,27] that results in monodisperse chains up to 50 monomers in length in high yield and relatively large batch sizes from hundreds of different readily available monomers. Polypeptoids therefore possess both the chemical diversity and the synthetic efficiency necessary for investigating the interplay of monomer sequence and thermal properties.

In this work, polypeptoids are shown to be thermally stable to very high temperatures and to have crystallinity which is easily controlled through the placement of sequence specific defects. We have synthesized a variety of polypeptoids of exactly 15 monomers in length to characterize their thermal properties and stability (Figure 1, Tables 1 and 2). Although 15 monomers is short compared to other polymers, this length allows for exquisite control over molecular sequence and, more importantly, enables the investigation of changes in crystalline structure with very subtle monomer changes. Many of these molecules exhibit crystalline structures with accessible melting transitions. To illustrate the tunability of these transitions, we have inserted defects into the peptoid homopolymers via a side-chain substitution at specific locations with the result that crystallization and hence the melting temperature are either decreased or suppressed completely. The type, content, and distribution of the defects have all been varied with exact control and monodispersity. This sequence specificity leads to increased understanding of the effects of these defects on the thermal behavior.

Experimental Methods

Synthesis. Polypeptoids were synthesized on a custom robotic synthesizer or a commercial Aapptec Apex 396 robotic synthesizer on 100 mg of Rink amide polystyrene resin (0.6 mmol/g, Novabiochem, San Diego, CA). All primary amine monomers, solvents, and reagents described here were purchased from commercial sources and used without further purification. The synthesis procedure was a modified version of methods previously described.[27] The Fmoc group on the resin was deprotected by adding 2 mL of 20% (v/v) piperidine/N,N-dimethylformamide (DMF), agitating for 20 min, draining, and washing with DMF. All DMF washes consisted of the addition of 1 mL of DMF, followed by agitation for 1 min (repeated five times). An acylation reaction was then performed on the amino resin by the addition of 1.0 mL of 1.2 M bromoacetic acid in DMF, followed by 0.18 mL of N,N-diisopropylcarbodiimide (DIC, 1.15 mmol, neat). The mixture was agitated for 20 min at room temperature,

drained, and washed with DMF. Nucleophilic displacement of the bromide with various primary amines (Table 1) occurred by a 1.0 mL addition of the primary amine monomer as a 1.0−1.5 M solution in N-methyl-2-pyrrolidone (NMP), followed by agitation for 60 min at room temperature. The monomer solution was drained from the resin, and the resin was washed with DMF as described above. The acylation and displacement steps were repeated until a polypeptoid of the desired length was synthesized. All reactions were performed at room temperature. All polypeptoids were acetylated on the resin after synthesis using a mixture (2.0 mL per 100 mg of resin) of 0.4 M acetic anhydride and 0.4 M pyridine in DMF for 30 min, followed by washing with DMF. Peptoid chains were cleaved from the resin by addition of 4.0 mL of a trifluoroacetic acid (TFA) cleavage cocktail for 20 min, which was then evaporated off under a stream of nitrogen gas. The composition of the TFA cleavage cocktail was 10% (v/v) TFA in dichloromethane for pNbu15, pNhx15, and pNia15. All other peptoids were cleaved with 95% (v/v) TFA in water. Following cleavage, peptoids were dissolved in 4.0 mL of either glacial acetic acid or appropriate acetonitrile/water mixtures and lyophilized twice to obtain a fluffy white powder.

Each polypeptoid was characterized by analytical reverse-phase HPLC using a C4 column (Vydac 214TP, 5 μm, 4.6 × 150 mm) on a Varian ProStar system (Palo Alto, CA). The column was maintained at 60 °C while a 30 min linear gradient of 5−95% solvent B in solvent A was used (solvent A = 0.1% TFA in water, solvent B = 0.1% TFA in acetonitrile). Electro-spray mass spectrometry was performed on an Agilent 1100 series LC/MSD trap system (Agilent Technologies, Santa Clara, CA). All peptoids were purified by reverse-phase prep HPLC on a Varian ProStar system equipped with a Varian model 345 UV−vis dual wavelength detector (214 and 260 nm) and a C4 column (Vydac HPLC Protein C4 column, 10−15 μm, 22 × 250 mm). pNpe15 required a linear gradient of 50−100% solvent B in solvent A over 40 min at a flow rate of 10 mL/min (solvent A = 0.1% TFA in water, solvent B = 0.1% TFA in 50:50 isopropanol:acetonitrile). All other peptoids used the same gradient but the same solvent system as that described for the analytical HPLC. pNoc15 was precipitated from acetonitrile and water.

Thermogravimetric Analysis. Samples were characterized using a TGA Q50 (TA Instruments, New Castle, DE) to investigate degradation temperatures by mass loss. Approximately 5.0 mg of lyophilized peptoid powder was placed on a 100 μL platinum sample pan. Samples were equilibrated at 30 °C for 20 min and then heated to 500 at 5 °C/min under a nitrogen atmosphere.

Differential Scanning Calorimtery. Differential scanning calorimetry (DSC) was carried out using a 2920 modulated DSC equipped with a DSC refrigerated cooling system (both TA Instruments, New Castle, DE). 4−10 mg of lyophilized peptoid powder was hermetically sealed into aluminum pans. Each sample was taken through three temperature cycles at heating and cooling rates of 5 °C/min. The first cycle from each sample was discarded in order to erase the thermal history.

<div align="center">

Table 2. Analytical Data for a Series of Peptoid 15-mers

</div>

polypeptoid	monomer sequence	X_n	molar mass (calc/obs)	purity (%)[a]
pNbu15	Ac-(Nbu)$_{15}$	15	1755.3/1755.8	78
pNhx15	Ac-(Nhx)$_{15}$	15	2177.2/2178.4	94
pNoc15	Ac-(Noc)$_{15}$	15	2598.0/2597.1	ND
pNia15	Ac-(Nia)$_{15}$	15	1965.5/1965.9	ND
pNpe15	Ac-(Npe)$_{15}$	15	2477.1/2477.6	ND
pNme15	Ac-(Nme)$_{15}$	15	1785.0/1788.6	78
pNpe-*co*-Npp2	Ac-(Npe)$_5$Npp(Npe)$_3$Npp(Npe)$_3$	15	2505.1/2505.0	96
pNpe-*co*-Npp4	Ac-(Npe)$_2$Npp(Npe)$_2$Npp(Npe)$_3$Npp(Npe)$_2$Npp(Npe)$_2$	15	2533.2/2533.2	99
pNia-*co*-Nhx2	Ac-(Nia)$_5$Nhx(Nia)$_3$Nhx(Nia)$_5$	15	1994.9/1994.2	ND
pNia-*co*-NHx4	Ac-(Nia)$_2$Nhx(Nia)$_2$Nhx(Nia)$_3$Nhx(Nia)$_2$Nhx(Nia)$_2$	15	2022.9/2022.2	99
pNia-*co*-Nme2a	Ac-(Nia)$_2$Nme(Nia)$_9$Nme(Nia)$_2$	15	1942.7/1945.2	96
pNia-*co*-Nme2b	Ac-(Nia)$_3$Nme(Nia)$_7$Nme(Nia)$_3$	15	1942.7/1943.4	97
pNia-*co*-Nme2c	Ac-(Nia)$_4$Nme(Nia)$_5$Nme(Nia)$_4$	15	1942.7/1943.4	96
pNia-*co*-Nme2d	Ac-(Nia)$_5$Nme(Nia)$_3$Nme(Nia)$_5$	15	1942.7/1942.2	93
pNia-*co*-Nme2e	Ac-(Nia)$_6$NmeNiaNme(Nia)$_6$	15	1942.7/1943.2	99
pNia-*co*-Nme4	Ac-(Nia)$_2$Nme(Nia)$_2$Nme(Nia)$_3$Nme(Nia)$_2$Nme(Nia)$_2$	15	1918.6/1918.0	89
pNle15	Ac-(Norleucine)$_{15}$	15	1713.3/1713.5	ND

[a] As determined by analytical HPLC of purified product (see Supporting Information for available traces). Ac = acetyl group, ND = not determined.

Polarized Optical Microscopy. Approximately 1−2 mg of lyophilized peptoid powder samples were placed between two glass slides secured to an Instec HCS302 heating stage (Boulder, CO) controlled by an Instec STC 200 temperature controller. The heating stage was further equipped with recirculating cooling water from a Neslab Coolflow CFT-25 (Thermo Scientific, Waltham, MA), and argon was continuously flowed over the sample to prevent burning. The sample apparatus was placed in an Olympus BX51 microscope, and data were collected using a 50× lens. Polarizers were placed over the lens to view the birefringence of the sample. Heating and cooling passes were executed at 5 °C/min to mimic the conditions of the DSC experiments.

X-ray Diffraction. X-ray diffraction (XRD) was performed at beamline 8.3.1 at the Advanced Light Source at Lawrence Berkeley National Laboratory. Samples were thermally annealed in a vacuum oven below their melting temperatures for 1−2 h, and 1−2 mg of the sample was then loaded onto a sample ring. X-rays of 11.11 keV were focused onto the sample, and a two-dimensional CCD array was used to collect the scattered X-rays after transmission through the sample. The signal was then radially integrated to obtain a 1D plot of intensity vs scattering angle.

Results and Discussion

Thermal Stability and Processability. Peptoid homopolymers are determined to be thermally stable to temperatures approaching 300 °C with thermal behavior that can be tuned by altering the monomer sequence within the chain. Furthermore, many of the monodisperse, 15-mer peptides crystallize with experimentally accessible thermal melting transitions. Figure 2 shows a representative XRD trace of a crystalline peptoid, pNbu15, as well as its DSC heating curve. X-ray powder diffraction obtained from the annealed peptoid shows two reflections in the ratio 1:2 at 44.35 and 22.09 Å, respectively. These reflections could suggest chain-folded lamellae with thicknesses that measure roughly three-fourths of the fully extended peptoid chain length, 58.1 Å, but this is difficult to imagine given the implied nonintegral folding. It is more likely that the peptoid chains are crystallizing such that one axis (the *c*-axis) of the unit cell is defined by the molecular length. XRD of three peptoids of various lengths supports this idea (see Supporting Information, Figure S1). The fact that the *c*-axis is shorter than the length of a fully extended peptoid chain indicates the chain conformation may not be completely *trans* zigzag. 2D NMR of achiral peptoid hexamers in solution has shown that the three types of rotamers in which the backbone amide bonds are

cis-dominated, *trans*-dominated, or a mixture are all equally likely.[28] If crystallization in the solid state does lead the chain to prefer a *trans* zigzag conformation, then the molecular axis would have to be tilted about 40° relative to the normal to the *c*-axis in the crystal to give dimensions consistent with the XRD.

Four additional wide-angle reflections are seen at *q* ratios of 1:2:3:4 at 13.4, 6.7, 4.5, and 3.5 Å, respectively. These peaks come from side chain organization (as inferred from Figure S1 in the Supporting Information), with the multiple reflections indicating that they are well-ordered. In addition, the broadening at the base of the 3*q* peak indicates overlap with another peak ~4.5 Å. Reflections at this spacing are common for every peptoid investigated, and it is thought that this corresponds to the spacing between peptoid chains.[29] Previously, Cui et al. indexed polypeptide single crystals to a hexagonal unit cell,[30] and while it is possible that the peptoid XRD peaks represent the 100, 200, 300, and 400 *hkl* reflections from such a unit cell, more reflections are necessary to confirm the assigned indices (see Supporting Information, Figure S2). In addition, diffraction of hexagonal packing usually shows a strong (110) reflection, which is not consistent with the data shown here.

pNbu15 melts over a narrow temperature range with a peak temperature of 168 °C and, upon cooling (not shown), recrystallizes at 150 °C. The transition is highly reversible for at least three temperature cycles.

Compared to other synthetic polyamides,[31,32] polypeptoids have much lower melting transitions, most likely due to the lack of hydrogen bonding in the N-substituted glycine backbone. By putting a side group on the backbone nitrogen, the main chain becomes devoid of hydrogen bond donors, whereas the amide linkages in nylons, aramids, or polypeptides allow hydrogen bonding to occur between adjacent chains. Such hydrogen bonding usually stabilizes the crystals and raises T_m. Hydrogen-bonding interactions also dominate the thermal properties of polypeptides.[33] Polyglycine, which can be thought of as a peptoid without a side chain on the backbone nitrogen, has been shown to degrade before melting.[33,34] A direct comparison of a polypeptoid and a polypeptide can be made between pNbu15 and pNle15. pNle15 has a side chain identical to that of pNbu15, but the side chain is covalently bonded to the backbone α-carbon instead of the amide nitrogen, thereby allowing the backbone hydrogen bonding characteristic of all polypeptides. Figure 2a illustrates that no melting transition was observed over the experimental temperature range for this peptide,
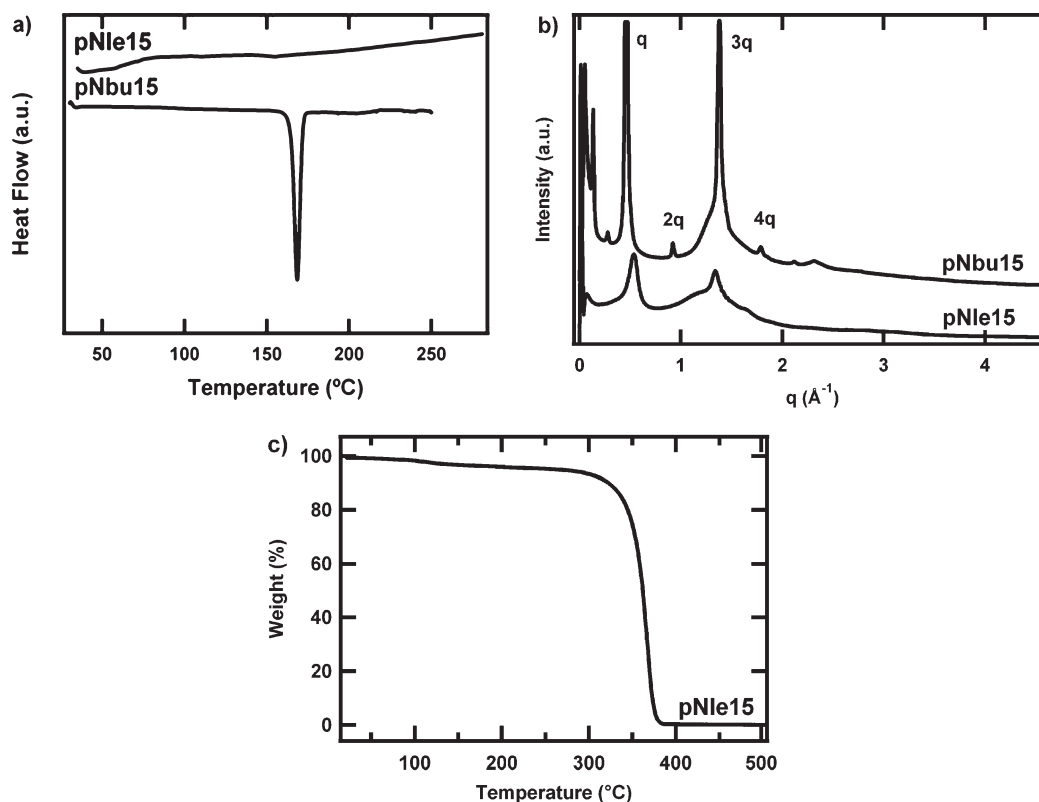
Figure 2. (a) DSC endotherms for a 15-mer polypeptoid (Nbu15) and its analogous polypeptide (pNle15). pNbu15 melts at a peak temperature of 168 °C, while pNle15 clearly shows no melting transitions over the experimental temperature range. (b) XRD spectra for pNbu15 and pNle15 indicate that the polypeptide does not anneal as easily as the polypeptoid due to decreased chain mobility from hydrogen-bonding effects. (c) TGA of pNle15 proves the polypeptide degrades before melting.

indicating that its crystal structure is likely stabilized by strong intermolecular interactions. In contrast, pNbu15 melts easily, as explained above. XRD (Figure 2b) indicates that thermal annealing does not enhance the crystal structure of pNle15, presumably because the chains do not have enough mobility to reorganize, while those of pNbu15 thermally anneal into well-organized crystals. Furthermore, thermogravimetric analysis (Figure 2c) confirms that pNle15 starts degrading at ∼320 °C before ever melting. Conversely, thermogravimetric analysis has confirmed the stability of all of the 15-mer polypeptoids synthesized up to ∼260 °C, leaving a region of thermal processability between the melting and degradation temperatures. The absence of strong intermolecular interactions suggests that polypeptoids may be suitable biologically inspired polymers for materials applications where processability and stability are necessary.

Controlling T_m by Varying Side Chains. Since the side-chain functionality is introduced via a primary amine submonomer, there are hundreds of moieties that can be incorporated into a polypeptoid. Such chemical diversity potentially enables one to design a polypeptoid with specifically tailored properties. Here, a series of polypeptoids with various alkyl side chain lengths are compared to observe the effect of side-chain chemistry on crystallization. Figure 3a presents the endotherms for polypeptoids with alkyl side chains 4 (pNbu15), 6 (pNhx15), and 8 (pNoc15) carbons long. Compared to pNbu15, which has a 4-carbon chain as a side group, longer alkyl chains lower the melting point. Adding two carbons to the side chain depresses the melting transition by almost 15 °C, while adding four carbons shifts the melting transition down by ∼30 °C. The latent heat of melting appears to also depend on side chain length, though it is unclear how the side chains are affecting the enthalpic contribution to the free

energy of crystallization. It is likely that longer, more flexible side chains prevent close crystalline packing of the molecules, thus making it easier to melt the material.

Except for pNhx15, the polypeptoids each show diffraction peaks at q and $2q$ in the small-angle region (Figure 3b). These peaks show a difference in location: 0.141 Å^{-1} (44.4 Å) for pNbu15 and 0.123 Å^{-1} (50.85 Å) for pNoc15. The small increase in d-spacing for pNoc15 may reflect that longer side chains push the polypeptoid chain into a more extended configuration or that they allow a crystal structure where the chain axis is not as tilted relative to the c-axis. The absence of the small-angle peaks in pNhx15 is an effect of the thermal history of the sample. Moving into the wide-angle region, each of these polypeptoids shows peaks with q ratios of 1:2:3:4 (Figure 3b), but both pNhx15 and pNoc15 have larger spacings than pNbu15. The major reflection at 0.353 Å^{-1} (17.8 Å) for pNoc15 represents a shift of about 4 Å relative to the same reflection seen for pNbu15 at 0.468 Å^{-1} (13.4 Å). The increase in d-spacing further confirms that these reflections come from side-chain crystallization and indicates that the longer side chains do indeed alter the spacing of the polypeptoid chains within the unit cell. Finally, both pNhx15 and pNoc15 show broadening and an increase in intensity around $4q$, suggestive of overlap with another peak centered around 4.5 Å as was discussed for pNbu15.

Conversely, the addition of bulkier side chains tends to drive the thermal transitions upward. Adding one carbon to pNbu15 to introduce a branch in pNia15 shifts the melting peak up to 178 °C. Whereas the addition of carbons in an *n*-alkyl conformation previously lowered the melting transition, the branched structure has the opposite effect, perhaps because the bulkier side group increases the overall stiffness
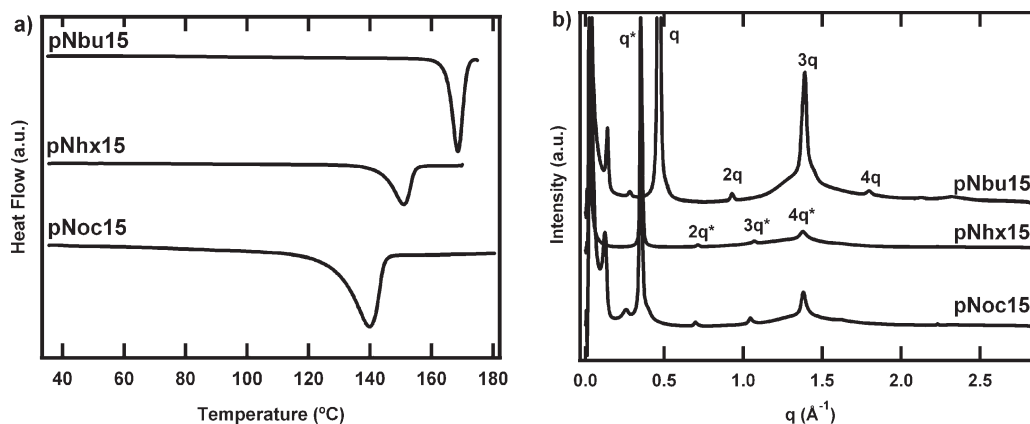
Figure 3. (a) DSC endotherms for three 15-mer peptoids with increasingly longer alkyl side chains: butyl (pNbu15), hexyl (pNhx15), and octyl (pNoc15). As side chain length increases, the melting temperature decreases. (b) XRD indicates that side chain length affects the spacings of the crystal lattice.
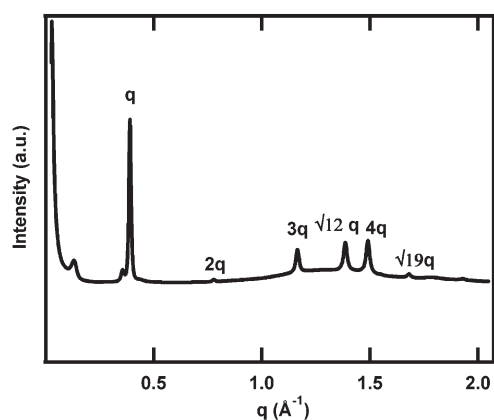

Figure 4. XRD pattern for pNpe15 shows several peaks, indicating a highly crystalline order.

Figure 5. (a) Polarized optical microscopy for pNpe15 exhibits strongly birefringent patterns at room temperature. (b) Upon heating past the melting transition, all birefringence is lost and an isotropic melt is observed.

Figure 6. DSC endotherms for pNpe15 illustrate the rate dependence of crystallization. After cooling from an isotropic melt at both 5 and 10 °C/min, the corresponding endotherms show that the peptoid continues to crystallize above its T_g before melting at 225 °C. For 1 °C/min, no further crystallization occurs upon heating.

of the polypeptoid chain. Introduction of an aromatic group in the side chain (pNpe15) has a more dramatic effect—the melting transition is driven up to 225 °C. The (001) spacing for pNpe15 is located at a q of 0.129 Å^{-1} (48.4 Å, Figure 4), which is extended relative to pNbu15 but still shorter than pNoc15. Unlike pNbu15, there is no second-order (002) reflection present, but there is an extraneous peak at 0.356 Å^{-1} whose origin is unclear. Because the extraneous peak is close to the major reflection at 0.37 Å^{-1}, which we believe stems from organization of the side chains, it may reflect the presence of two competing side-chain structures within the crystalline domains. In addition to the wide-angle diffraction peaks seen at the q ratios of 1:2:3:4, pNpe15 also diffracts at the additional spacings of 4.5 and 3.7 Å (Figure 4), which are approximately $12^{1/2}q$ and $19^{1/2}q$, respectively. Both of these reflections are allowed in a hexagonal unit cell (among others) and so unfortunately do not contribute any additional information about the crystalline lattice of the peptoid. However, it should be noted that diffraction at similar spacings were seen by Nam et al. in a crystalline, two-dimensional peptoid sheet.[29] The spacing at 4.5 Å was attributed to chain−chain spacing (as previously mentioned), while the spacing at 3.7 Å corresponds to the spacing between each monomer residue along the peptoid chain in an extended conformation. The diffraction could therefore be further evidence of an extended chain conformation for pNpe15. Besides the sharp diffraction pattern and the narrow and well-defined melting peak, strongly birefringent patterns in POM (Figure 5) confirm that pNpe15 is strongly crystalline
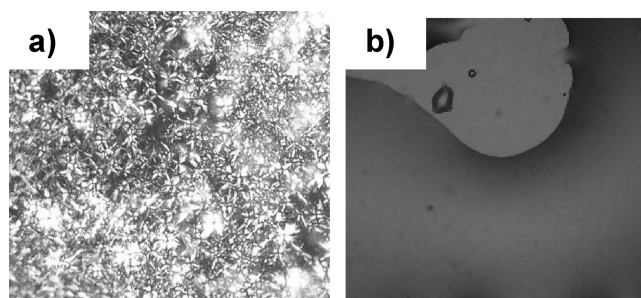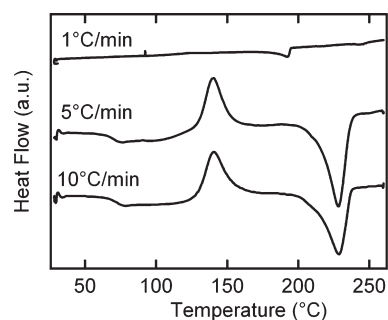
at room temperature. This crystalline phase is present until melting into an isotropic phase at 225 °C, a high temperature relative to the melting points of the other polypeptoids synthesized.

The kinetics of crystallization have a significant effect on the thermal behavior of pNpe15. At faster cooling rates, the material is locked into a solid conformation before it is able to fully crystallize. This is evidenced by the lack of a definitive crystallization peak in the cooling trace of the DSC (not shown). However, upon heating, the chains become mobile again and crystallize before melting at 225 °C (Figure 6). Slower temperature ramps allow the material to crystallize fully upon cooling, and there is no subsequent further crystallization upon reheating. The cold crystallization exotherm is

2 Defect Scheme
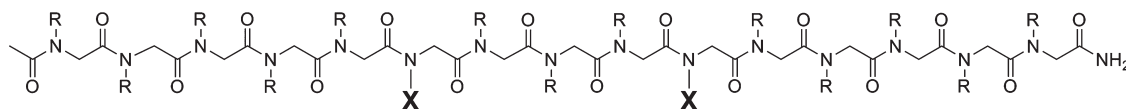
4 Defect Scheme
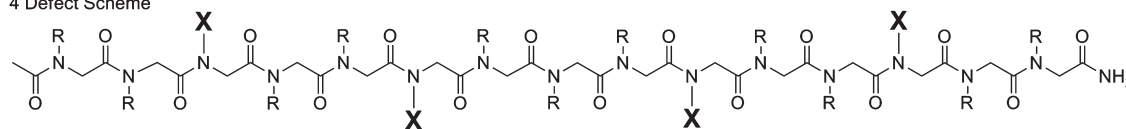
No. defects	R=	X=	Name
2			pNia-co-Nme2d
2			pNia-co-Nhx2
2			pNpe-co-Npp2
4			pNia-co-Nme4
4			pNia-co-Nhx4
4			pNpe-co-Npp4

Figure 7. "Defects" were inserted along a 15-mer peptoid chain according to two schemes. X denotes defects; R denotes side chains, as listed in the table.

different from a glass transition temperature which can also be seen in DSC traces upon heating. A glass transition reflects the increased motion of the chains relative to each other and is seen as an inflection point in the DSC trace. Recrystallization, however, is seen as an exothermal peak and indicates the reordering of the chains into an organized lattice. The passage of the T_g in this case allows the recrystallization to occur.

Controlling T_m with Sequence Defects. Sequence control provides an additional handle for tuning the thermal transitions of polypeptoids. It is well-known that increasing comonomer content decreases the melting temperature for classical polymers such as polylactides[13,35] and polyethylenes.[2] In general, the comonomer content is related to the average length of a crystallizable sequence in the polymer, and the shorter that length, the lower the melting temperature of the copolymer. However, in most synthetic polymers this average sequence length can be difficult to control since it is dependent upon the molar ratio of the two monomers and their reactivity ratio, as described by Mayo and Lewis.[36] The stepwise synthesis of polypeptoids enables the average sequence length to be specified by inserting an exact number of defects per chain.

We have designed two symmetric yet arbitrary monomer sequences to investigate the effect of comonomer units on crystallinity for two polypeptoids: pNia15 and pNpe15, which as previously discussed have very different thermal behavior. To these two homopolymers, defects consisting of monomers with slight differences, particularly in terms of side chain bulk, were added. Chains with two defects contained monomer substitutions at positions 6 and 10, while chains with four defects contained substitutions at positions 3, 6, 10, and 13 (Figure 7). In the case of the pNia15 polymer,

two defects were made: an unbranched alkyl side chain two carbons longer than the hompolymer side chain and a methoxyethyl side chain. Sequences are tabulated in Table 2. In the case of pNpe15, the defect side chain is virtually identical to the homopolymer side chain, but the phenyl ring is spaced one more alkyl unit away from the chain. Thus, the side chain imparts not a chemical defect but rather a spatial one.

In agreement with the work done on random copolymers, we have found that the introduction of defects at precise locations in the polymer sequence (as a side-chain substitution) allows crystallization and hence the melting temperature to be reduced for pNia15 when the defect is *N*-hexylglycine. *N*-Hexylglycine defects introduced to pNia15 homopolymer depress the melting transition by up to 20 °C (Figure 8a). Increasing the number of defects drives the melting temperature down further, indicating that the substitutions disrupt the thermodynamics of polypeptoid crystallization. In addition, the disappearance of higher-order XRD reflections for both q^* (the low angle reflection, Figure 8b inset) and q (Figure 8b) suggests that the copolymers' crystal organization is disrupted relative to the pNia15 homopolymer. The peak just past $3q$ at 1.36 Å^{-1}, however, persists for all polypeptoids. This peak corresponds to a spacing of 4.6 Å, which may be the chain–chain spacing, as previously mentioned in the discussion above. It is worthy to note that all variations of the pNia15 copolypeptoid crystallized, even for an average sequence length of 2.2 pNia15 units. This number is low compared to a more traditional system such as ethylene copolymers, where the critical sequence length for crystallization lies between 6 and 25.[37] Even for polyethylenes with a short chain branch introduced at precisely every fifth carbon (yielding an ethylene run
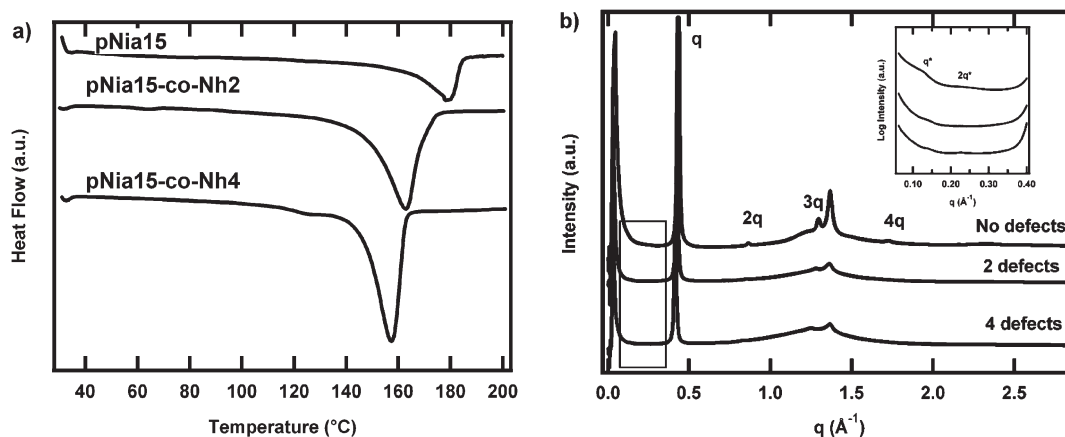
Figure 8. (a) DSC traces for pNia15, containing 0, 2, and 4 defects of Nhx. Increasing the number of defects disrupts crystallization and suppresses the melting point. (b) XRD patterns for pNia15 homopolymers with 0, 2, and 4 defects. All three samples show nearly identical spectra.
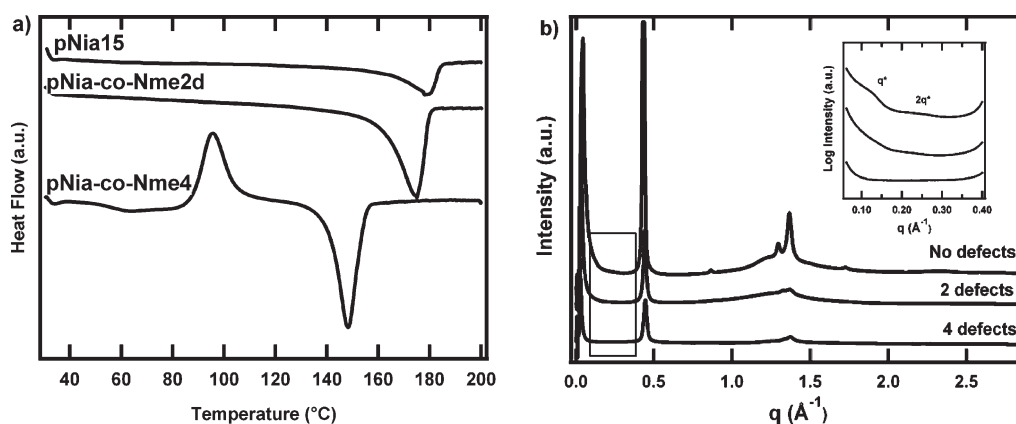

Figure 9. (a) DSC endotherms for pNia15 with 0, 2, and 4 defects of Nme. The exothermic peak in pNia-*co*-Nme4 is due to cold crystallization of the polypeptide. (b) XRD patterns for pNia15 homopolymers with 0, 2, and 4 Nme defects. It is obvious that the Nme defects suppress crystallization.

length of four carbons), the resulting copolymer is amorphous.[22] The possibility of defect cocrystallization within the peptoid chain may be one reason that such short lengths of pNia15 units can still crystallize.

N-2-Methoxyethylglycine defects were also inserted into the pNia15 homopolymer. The methoxyethyl branch is chemically different from the isoamyl side chain of the homopolymer. *N*-2-Methoxyethylglycine monomer substitutions inserted at the same positions (Figure 7) altered the thermodynamics of crystallization in a similar way to the *N*-hexylglycine defects. XRD spectra (Figure 9b) for these copolymers once again show fewer higher order reflections than the spectrum of the homopolymer, though the peak at 1.36 Å still persists. The DSC endotherms (Figure 9a) show that the depression of the melting temperature is approximately the same order of magnitude as that of the *N*-hexylglycine copolymers.

The thermal behavior of the pNia15 copolymers differs from the behavior predicted by Flory's theory of crystallization[10] (previously shown as eq 1). The melting temperatures calculated from this equation are higher than the observed values, as shown graphically in Figure 10a. The main difference between the predicted melting temperatures and the observed melting temperatures is that the topographic defects used to suppress crystallization in this polypeptoid experiment are not randomly placed and, as a result, may actually participate in and affect the crystal packing, while Flory's theory assumes exclusion of the defect from the crystal lattice. In addition, Flory's theory takes the crystal

structures to be at total equilibrium, a situation that is difficult to achieve even with extremely slow crystallization conditions. The enthalpy of melting of these polypeptoids increases when a greater number of defects are present in the chain (Figure 10b). It is interesting to note that if these are equilibrium melting temperatures, then the entropy of melting must also increase in order for the melting temperature to decrease with respect to the homopolymer . However, since the entropy of melting is not measurable, we can only postulate its increase. Although our peptoid system is markedly different from that derived for Flory's treatment, it is interesting for comparison's sake that the basic form of Flory's theory still holds for the peptoid copolymers: increasing defect content depresses the melting temperature.

Interestingly, defects introduced into pNpe15 homopolymer disrupted the crystal structure nearly completely. No birefringent patterns were seen in POM for any of the copolymers, and the DSC traces show a drastic reduction in the peak size for melting and recrystallization to the point of complete disappearance, as shown in Figure 11a. Furthermore, the XRD patterns (Figure 11b) show broad, diffuse scattering consistent with a lack of crystalline order. Both defected polypeptoids show two peaks: one centered around 0.4 Å^{-1} and one centered around 1.3 Å^{-1}. It is possible that there may be some weak ordering of the side chains and the chain−chain spacings at 0.4 and 1.3 Å^{-1}, respectively. The lack of sharp diffraction peaks suggests that the crystalline packing of the pNpe15 homopolymer is strongly sensitive to the placement of the aromatic rings, and the addition of
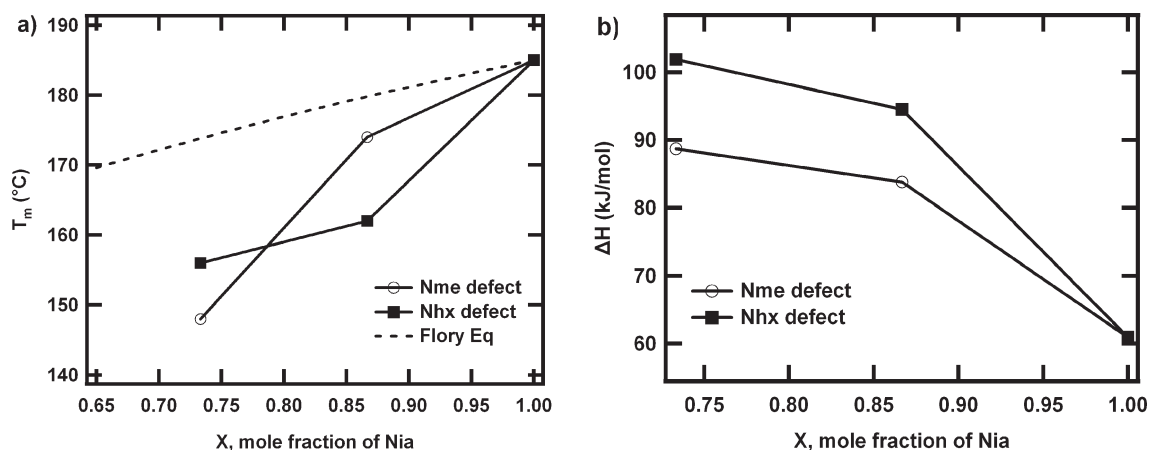
Figure 10. (a) Melting point comparison for pNia15 defected with Nhx and Nme graphed by mole fraction. Dotted line represents the melting points predicted by the Flory equation. (b) Enthalpies of melting for the same defected pNia15 polymers. As the defect content increases, the heat of melting also increases.
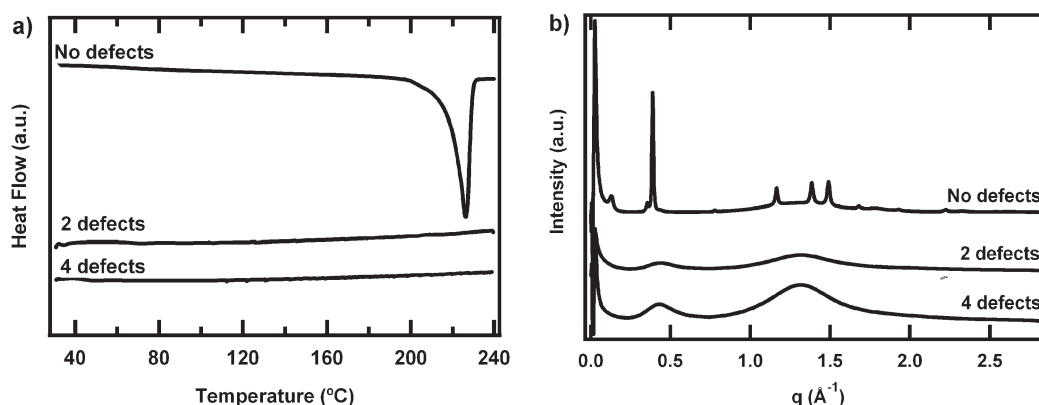

Figure 11. (a) DSC traces for pNpe15 containing 0, 2, and 4 defects. Increasing the number of defects disrupts crystallization completely. (b) XRD patterns for pNpe15 homopolymers with 0, 2, and 4 defects. The traces for samples with defects indicate an amorphous solid.

Table 3. pNia15 Copolymers with Various Sequence Distributions of Two Defects[a]

polypeptoid	T_m (°C)	ΔH (J/g)	avg Nia length	sequence
pNia-*co*-Nme2a	174	58.3	4.3	X X O X X X X X X X X X O X X
pNia-*co*-Nme2b	166	48.9	4.3	X X X O X X X X X X X O X X X
pNia-*co*-Nme2c	174	51.5	4.3	X X X X O X X X X X O X X X X
pNia-*co*-Nme2d	170	41.9	4.3	X X X X X O X X X O X X X X X
pNia-*co*-Nme2e	173	35.5	4.3	X X X X X X O X O X X X X X X

[a] O denotes a defect; X denotes a Nia monomer.

defects with an additional chemical moiety prevents the chains from aligning in any ordered way. It remains to be seen whether a less bulky defect (i.e., one without an aromatic ring) would still allow the pNpe copolymer to crystallize.

Controlling the Distribution of Sequence Defects. Not only can one exert exact control over the amount of defects per chain, but one can also control the pattern of defects within the peptoid monomer sequence. Unlike random copolymerizations, polypeptoids are synthesized such that a monodisperse batch of uniform sequence is obtained, therefore enabling direct comparisons between various distributions for peptoids with exactly the same number of defects. Recent progress has been made in the sequence control of polyethylene copolymers containing chlorines such that the chlorine atoms can be precisely limited to every *n*th carbon.[24] While this is a significant achievement for polymers of high molecular weight, polypeptoids offer greater freedom over the distribution of the "comonomer". A series of defected pNia15 polymers, all with exactly two defects of Nme each, are

shown in Table 3. The position of these two defects varies within the peptoid chain between each polymer, giving each copolymer different run lengths of Nia monomers or different "degrees of blockiness".[38] The exact sequences are tabulated in Table 2; the sequences have been reproduced pictorially in Table 3.

Although all pNia15 copolymers in this series have the same average Nia length (since all copolymers have exactly 2 defects for 15 monomer spaces), there are significant differences in the enthalpy of melting. It appears that the polymers with the defects located toward the center of the chain have the lowest enthalpies of melting, though their melting temperatures are not significantly different from those of the other copolymers. The XRD spectra (Figure 12) for all copolymers are extremely similar, though there are subtle differences in the location of the (001) peak and in the broadness of the peak at a q of 1.4 Å^{-1}. The copolymers with the most asymmetric blocks of Nia side chains have sharper (001) reflections at spacings of 44.9, 45, and 44.2 Å
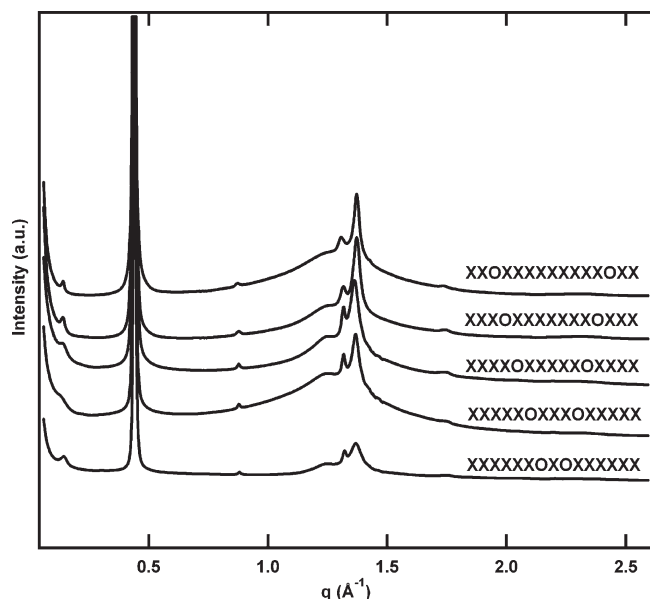
Figure 12. XRD patterns for a series of pNia15 copolymers, all with two defects each. The location of the defects does not appear to affect the crystalline packing of the polymer in a qualitative way, though the location of the (001) peak at low *q* shifts slightly and broadens for the third and fourth spectra.

(the first, second, and fifth spectra in Figure 12), while the copolymers with more evenly spaced blocks of Nia side chains have broader (001) reflections at spacings of 46.1 and 48.3 Å. It is possible that in the more asymmetric copolymers only the longest blocks of Nia are participating in crystallization (and leaving out the ends or the middle in the fifth case), whereas in the more evenly spaced copolymers, it is more energetically favorable for the entire chain to crystallize. In general, however, all of the reflections after the (001) are extremely similar for the copolymers. These preliminary experiments raise several questions, such as whether a more asymmetric distribution would have a larger effect on thermal behavior (all sequences investigated are symmetric). The peptoid system promises to be ideal for exploring the effects of sequence distribution on physical properties.

Conclusions

The thermal behavior of various polypeptoids exactly 15 monomers in length has been investigated. In contrast to polypeptides, several polypeptoids were found to melt and recrystallize at experimentally accessible temperatures, most likely due to the lack of intermolecular hydrogen bonding. Polypeptoid crystallization was controlled by changing the side chain as well as by introducing sequence specific defects into polypeptoid homopolymers (via side-chain substitutions). As expected, increasing the number of defects depresses the melting temperature, though in some cases, it suppresses crystallization completely. The location of these defects can be specified *exactly*, and a series of polypeptoid copolymers with exactly two defects in various distributions were synthesized. While the crystal structure and melting temperatures were slightly affected by the defect distribution, the enthalpies of melting varied significantly among the polypeptoids investigated. The sequence specificity and thermal stability of polypeptoids demonstrated in this work lay the foundation for polypeptoids as novel, biologically inspired polymers for materials applications.

Supporting Information Available: XRD for three polypeptoids of 6, 15, and 30 monomers and analytical HPLC traces for listed polypeptoids. This material is available free of charge via the Internet at http://pubs.acs.org.

Note Added after ASAP Publication. This article posted ASAP on June 9, 2010. Figures 2, 6, and 7 have been revised. The correct version posted on June 14, 2010.

References and Notes

(1) Kint, D. P. R.; Munoz-Guerra, S. *Polym. Int.* **2003**, *52* (3), 321–336.
(2) Alamo, R. G.; Mandelkern, L. *Thermochim. Acta* **1994**, *238*, 155–201.
(3) Zhang, M.; Lynch, D. T.; Wanke, S. E. *Polymer* **2001**, *42* (7), 3067–3075.
(4) Baratian, S.; Hall, E. S.; Lin, J. S.; Xu, R.; Runt, J. *Macromolecules* **2001**, *34* (14), 4857–4864.
(5) Crist, B.; Howard, P. R. *Macromolecules* **1999**, *32* (9), 3057–3067.
(6) Hauser, G.; Schmidtke, J.; Strobl, G. *Macromolecules* **1998**, *31* (18), 6250–6258.
(7) Boz, E.; Nemeth, A. J.; Wagener, K. B.; Jeon, K.; Smith, R.; Nazirov, F.; Bockstaller, M. R.; Alamo, R. G. *Macromolecules* **2008**, *41* (5), 1647–1653.
(8) Sfatos, C. D.; Shakhnovich, E. I. *Phys. Rep.* **1997**, *288* (1−6), 77–108.
(9) Madkour, T. M.; Azzam, R. A.; Mark, J. E. *J. Polym. Sci., Part B: Polym. Phys.* **2006**, *44* (18), 2524–2541.
(10) Flory, P. J. *Trans. Faraday Soc.* **1955**, *51* (6), 848–857.
(11) Paul, J. F. *J. Chem. Phys.* **1949**, *17* (3), 223–240.
(12) Burfield, D. R. *Macromolecules* **1987**, *20* (12), 3020–3023.
(13) Sarasua, J. R.; Prud'homme, R. E.; Wisniewski, M.; Le Borgne, A.; Spassky, N. *Macromolecules* **1998**, *31* (12), 3895–3905.
(14) Richardson, M. J.; Flory, P. J.; Jackson, J. B. *Polymer* **1963**, *4* (2), 221–236.
(15) Alizadeh, A.; Richardson, L.; Xu, J.; McCartney, S.; Marand, H.; Cheung, Y. W.; Chum, S. *Macromolecules* **1999**, *32* (19), 6221–6235.
(16) Cheng, S. Z. D.; Janimak, J. J.; Zhang, A. Q.; Hsieh, E. T. *Polymer* **1991**, *32* (4), 648–655.
(17) Hosoda, S. *Polym. J.* **1988**, *20* (5), 383–397.
(18) Paul, S. *Polym. Int.* **1996**, *40* (2), 111–122.
(19) Sanchez, I. C.; Eby, R. K. *Macromolecules* **1975**, *8* (5), 638–641.
(20) Adisson, E.; Ribeiro, M.; Deffieux, A.; Fontanille, M. *Polymer* **1992**, *33* (20), 4337–4342.
(21) Baughman, T. W.; Wagener, K. B. Recent advances in ADMET polymerization. In *Metathesis Polymerization*; Springer-Verlag: Berlin, 2005; Vol. *176*, pp 1−42.
(22) Rojas, G.; Berda, E. B.; Wagener, K. B. *Polymer* **2008**, *49* (13−14), 2985–2995.
(23) Sworen, J. C.; Smith, J. A.; Berg, J. M.; Wagener, K. B. *J. Am. Chem. Soc.* **2004**, *126* (36), 11238–11246.
(24) Alamo, R. G.; Jeon, K.; Smith, R. L.; Boz, E.; Wagener, K. B.; Bockstaller, M. R. *Macromolecules* **2008**, *41* (19), 7141–7151.
(25) Kirshenbaum, K.; Zuckermann, R. N.; Dill, K. A. *Curr. Opin. Struct. Biol.* **1999**, *9* (4), 530–535.
(26) Simon, R. J.; Kania, R. S.; Zuckermann, R. N.; Huebner, V. D.; Jewell, D. A.; Banville, S.; Ng, S.; Wang, L.; Rosenberg, S.; Marlowe, C. K.; Spellmeyer, D. C.; Tan, R. Y.; Frankel, A. D.;

Santi, D. V.; Cohen, F. E.; Bartlett, P. A. *Proc. Natl. Acad. Sci. U.S.A.* **1992**, *89* (20), 9367–9371.

(27) Figliozzi, G. M.; Goldsmith, R.; Ng, S. C.; Banville, S. C.; Zuckermann, R. N. *Methods Enzymol.* **1996**, *267*, 437–447.

(28) Wu, C. W.; Sanborn, T. J.; Huang, K.; Zuckermann, R. N.; Barron, A. E. *J. Am. Chem. Soc.* **2001**, *123* (28), 6778–6784.

(29) Nam, K. T.; Shelby, S. A.; Choi, P. H.; Marciel, A. B.; Chen, R.; Tan, L.; Chu, T. K.; Mesch, R. A.; Lee, B.-C.; Connolly, M. D.; Kisielowski, C.; Zuckermann, R. N. *Nature Mater.* **2010**, *9* (5), 454−460.

(30) Cui, H. G.; Krikorian, V.; Thompson, J.; Nowak, A. P.; Deming, T. J.; Pochan, D. J. *Macromolecules* **2005**, *38* (17), 7371–7377.

(31) Ke, B.; Sisko, A. W. *J. Polym. Sci.* **1961**, *50* (153), 87.

(32) Xenopoulos, A.; Wunderlich, B.; Subirana, J. A. *Eur. Polym. J.* **1993**, *29* (7), 927–935.

(33) Lotz, B. *J. Mol. Biol.* **1974**, *87* (2), 169.

(34) Franco, L.; Xenopoulos, A.; Subirana, J. A.; Puiggali, J. *J. Polym. Sci., Part A: Polym. Chem.* **1995**, *33* (4), 727–741.

(35) Sodergard, A.; Stolt, M. *Prog. Polym. Sci.* **2002**, *27* (6), 1123–1163.

(36) Mayo, F. R.; Lewis, F. M. *J. Am. Chem. Soc.* **1944**, *66*, 1594–1601.

(37) Chen, Q.; Luo, H. J.; Yang, G. A.; Xu, D. F. *Polymer* **1997**, *38* (5), 1203–1205.

(38) Khokhlov, A. R.; Khalatur, P. G. *Physica A* **1998**, *249* (1−4), 253–261.